

Etching characteristics of si wafer thinning in HF/H₂O binary solution for microelectronic and nanopackaging applications

R. Ariff^{a,b}, C. K. Sheng^{a,*}

^a*Faculty of Science and Marine Environment, Universiti Malaysia Terengganu 21030 Kuala Nerus, Terengganu, Malaysia.*

^b*Faculty of Ocean Engineering Technology and Informatics, Universiti Malaysia Terengganu 21030 Kuala Nerus, Terengganu, Malaysia.*

The wet etching of silicon surfaces by the use of acidic or fluoride solutions is of both technological and fundamental significance, which is essentially to be applied to produce a reliable silicon chip at desired thickness for microelectronic packaging. In this work, we have investigated the wet etching effect on thickness dissipation, weight loss, etching rate, surface morphology and crystalline nature of Si wafer immersed in the 48 % HF/water solution. The etch rate was ascertained from the variation of weight loss and depth etched against time. The results show that the thickness reduction and weight loss of silicon increases as the etching time increases. Roughened surface is observed on the etched Si wafer surface under the high-resolution optical microscope. From the XRD analysis, it shows that the crystalline peak intensity of silicon becomes weaker after etching, implying the reduced light scattering from the formed amorphous structure surface on the Si substrate. After all, this finding can be valuably referred to produce a reliable Si thin wafer, which is crucial in thinner microelectronic devices fabrication and nanopackaging, and in turn reduces environmental pollution and energy consumption for future sustainability.

(Received March 27, 2021; Accepted July 7, 2021)

Keyword: Wet etching, Si, Etch rate, HF, H₂O

1. Introduction

The new microelectronic products require wafer to be thinned at the desired thickness for a wide variety of new microelectronic product fabrications, such as power and optoelectronic devices. Production of a new semiconductor silicon (Si) wafer for thinner packaging is usually costly that requires high energy consumption and also causes the environmental pollution problem. Mechanical grinding and plasma dry etch are the most common technique for wafer thinning due to its high thinning rate. However, the residual defect on the wafer surface that leads to wafer breakage with a rough surface still be produced by these techniques. This issue can be simply solved by using the wet etching method to produce the silicon chip at the desired thickness. Wafer that have been thinned using a wet etch process will have less stress compared with mechanical grinding. Wafer breakage will be reduced and after dicing the chips, it will have fewer cracks [1-6].

Eyad et al. [7] has reported the influence of IPA concentration and the etching time on the pyramidal surface structures formation on etched mc-Si in alkaline solutions. Narasimha et al. [8] has studied the etching behavior of Si in 20 wt% KOH with addition of hydroxylamine for the fabrication of bulk micromachined MEMS, in which the etch rate and undercutting are improved significantly. Stable etch rate is very useful to achieve larger etch depth in less time in comparison to common etchant. In this study, the wet etching was performed on the silicon wafer immersed in the HF and water solution at HF concentration of 48 wt%. The thickness reduction , weight loss, etch rate, surface morphology and crystal structure of the silicon wafer were determined by using the analytical semi-micro balance, digital micrometer, optical microscope and X-Ray diffractometer (XRD), respectively.

* Corresponding author: chankoksheng@umt.edu.my

2. Materials, preparation and characterizations

The chemicals of HF (Merck, German) and distilled water were used without any purification. Prior to etching, the Si wafer underwent solvent cleaning process. The main purpose was to remove the oil and organic residues on its surface. Firstly, the wafer was cleaned using acetone, in which the acetone in the beaker was heated at temperature up to 55 °C. However, the acetone leaves its own residue and therefore the ethanol was used to clean the acetone residue. The wafer was then placed into the water bath contained ethanol for 10 minutes. Then the wafers were removed from the bath and rinsed in distilled water. The wafers were dried in air for one day before the etching.

For the etching process, the Si wafer was dipped into the HF etchant/water solution at 48% concentration with the time interval of ten minutes up to 1 hour. The wafer was then washed with distilled water and dried by air before further characterizations. Analytical semi-micro balance (model GH-202 series) was used to measure the weight loss while the digital micrometer (model DTG03L) was used to determine the thickness reduction of silicon wafer. Optical microscope (model TM-1000 Hitachi) and XRD (model MiniFlex II) were used respectively to study the surface morphology and crystallinity of the silicon wafer before and after the etching. The variation of total thickness reduction and weight loss was calculated based on the equations below:

$$XL = X_f - X_i \quad (1)$$

$$WL = W_f - W_i \quad (2)$$

where XL and WL indicate the thickness and weight loss, respectively while the X_f , X_i , W_f , W_i denote the initial and final thickness, initial and final weight, respectively. The etch rate was then determined by the variation of total thickness reduction and weight loss against time using the following equations:

$$\text{Etch rate for thickness reduction} = \frac{XL}{t} = \frac{X_f - X_i}{t} \quad (3)$$

$$\text{Etch rate for weight loss} = \frac{WL}{t} = \frac{W_f - W_i}{t} \quad (4)$$

3. Results and discussion

Initially, the silicon wafers were etched with HF concentrations of 48% for an hour at time interval of 10 minutes. Fig. 1 shows the thickness reduction versus etching time for the silicon etched in 48% HF solution. From the figure, the thickness reduction of silicon increases with increasing etching time. As in detail, the thickness reduction caused by HF etchant begins to increase from 10 to 20 minutes etching time and becomes constant for the subsequent 30 minutes etching duration. After that, it shows a significant increase until the entire etching period. The highest thickness reduction recorded for the silicon wafer is 20 µm as contributed by HF etchant for 60 minutes etching period. The present result demonstrates that the thinning effect occurred on the Si wafer could be essentially utilized in micro-electronics devices packaging [9].

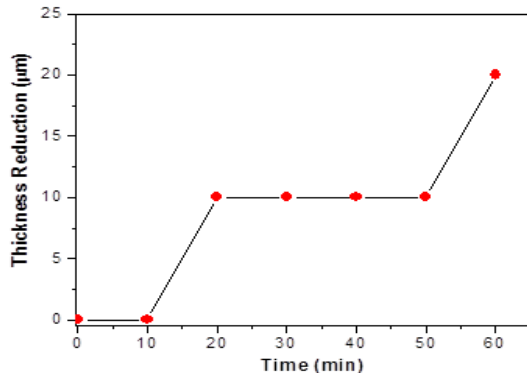


Fig. 1. Thickness reduction versus etching time for the Si immersed in HF.

Fig. 2 illustrates the weight loss as the etching time progressed for the silicon etched in HF/water solution. Clearly, it shows that the weight loss is increased as the etching time increases. The highest weight loss was recorded to be 2.6 mg for the silicon etched by HF solution. According to the figure, the weight loss caused by HF shows a rapid increase after 10 minutes of etching and then rises gradually with time after etching for 20 minutes until the entire process. This characteristic denotes the desired silicon leftover could be collected in powder form by selecting the appropriate etching time, whereby this type of product is useful for nanomaterial fabrication with potential optoelectronic application.

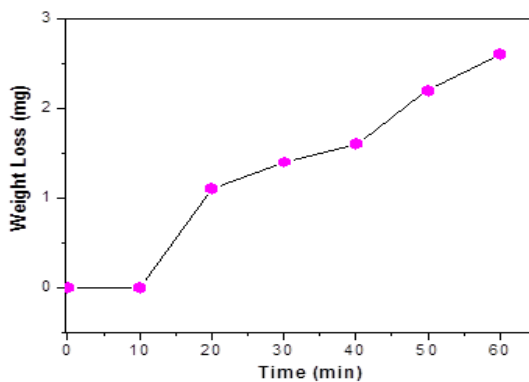


Fig. 2. Weight loss versus etching time for the Si etched by HF.

In this study, the etch rate was determined based on the variation of thickness and weight of silicon wafer against time by using equation (3) and equation (4). Fig. 3 shows the etch rate determined from thickness reduction varies with time for the present sample. The range of thickness reduction etch rate of silicon wafer is in between $0.20 \mu\text{m}/\text{min}$ to $0.50 \mu\text{m}/\text{min}$. From the figure, the etch rate shows a noticeable increase after 10 minutes of etching in the beginning of the process. Afterwards, the etch rate decreases uniformly with the extended time. This feature implies that a controllable silicon thinning process can be achieved in order to obtain a desired silicon wafer thickness [9]. On the other hand, the etch rate of weight loss versus time for the present sample is depicted in Fig. 4. Interestingly, an identical trend can also be observed for the etch rate determined from the weight loss by comparing to the one obtained from thickness reduction. This finding reflects that the rate of reaction becomes slower and a suitable etching speed can be set for wafer thinning process in order to meet the required fabrication condition.

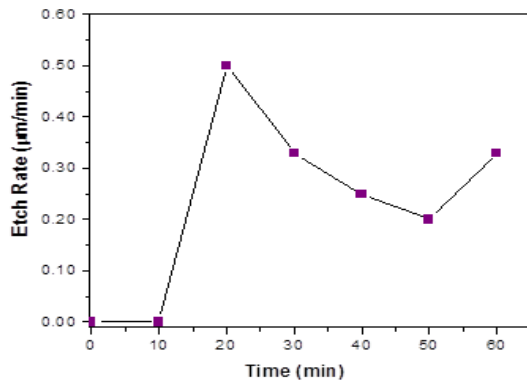


Fig. 3. Etch rate of thickness reduction for the silicon etched by HF.

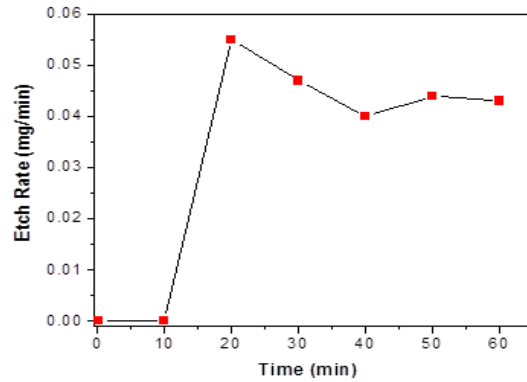


Fig. 4. Etch rate of weigh loss for the silicon etched by HF.

In this research, the surface morphology image was studied by using optical microscope at 100X magnification as presented in Fig. 5. From the figure, it can be seen that the surface morphology of the silicon wafer shows a discernible change after an hour of etching process. As compared to the one before etching, the etched silicon wafer surface becomes darker and rougher with the presence of larger microspores on the surface. This observation can be explained by the oxidation of silicon surface by holes injection, and hence leading to a faster dioxide dissolution by HF on Si [10]. Furthermore, the polishing efficiency as reported by Sheng et al. [9] does not occur in the present sample. This is based on the fact that the HF is a weak acid, especially when presents alone in a very small concentrations, it does not completely dissociate into H⁺ and F⁻ ion in water [11]. Nevertheless, the etching process would become active when both acids of HF and HNO₃ are mixed together, depending on the etchant concentration used and the initial thickness of silicon wafer to be etched [12]. Moreover, the formation of darker and rougher surface after etching is suitable for light trapping to improve the light absorption and power conversion efficiency, which is essential for solar device fabrication.

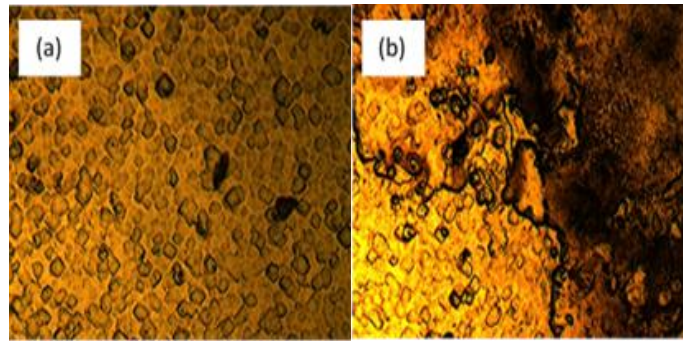


Fig. 5. Surface morphology of silicon wafer (a) before and (b) after an hour etching in HF/H₂O solution.

The crystalline nature of the sample was further determined by XRD and the result is shown in Fig. 6. The peaks are observed in the range from 69° to 70°. From the figure, two main peaks emerged in the XRD pattern may correspond to the reflectance from the planes of bulk and the polished Si surface. Also, the peak intensity of the pure silicon was determined much higher than etched Si. This effect indicates that the rougher surface produced might reduce the lattice light scattering and hence decreases the light intensity. Another reason for this is the creation of a significant amount of amorphous SiO₂ on the Si surface after etching. Additionally, both peaks present in the diffractogram shift slightly to a lower value of 2θ after etching, implying higher interplaner spacing values of atomic layers in silicon, which is essential in integrated circuits fabrication [13-17].

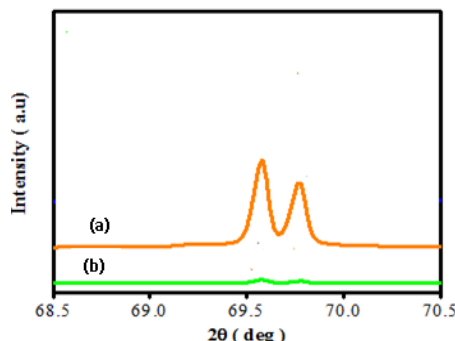


Fig. 6. XRD pattern of Si (a) before etching and (b) after etching with HF/H₂O.

5. Conclusion

In conclusion, it is worth to summarize that the present finding denotes a flexibly real-time controllable thinning effect on the silicon wafer to a desired thickness after etching in the water containing HF solutions. The result shows that the etch rate increases during the initial stage but decreases after the remaining etching time. After etching, the surface of silicon wafer becomes darken and roughen with reducing light scattering from the amorphous layer that is useful for solar device absorption. The present finding indicates that the etched Si can be potentially fitted into thinner packaging especially for optoelectronic products fabrication.

Acknowledgements

The authors would like to thank the Faculty of Science and Marine Environment, Faculty of Ocean Engineering Technology and Informatics, Universiti Malaysia Terengganu and the

Malaysian Government for the assistance and support in conducting this work through the research grant (FRGS-59122).

References

- [1] T. J. E. Dwight, C. K. Sheng, M. I. N. Isa, Malaysian J. Anal. Sci. **15**, 227 (2011).
- [2] E. S. Kooij, K. Butter, J. J. Kelly, Electrochem. Solid-State Lett. **2**, 178 (1999).
- [3] C. K. Sheng, W. M. M. Yunus, W. M. Z. W. Yunus, Z. A. Talib, A. Kassim, Physica B Condens. Matter **403**, 2634 (2008).
- [4] R. C. Prosenjit, Handbook of microlithography, micromachining and microfabrication, Volume 2: micromachining and microfabrication, Society of Photo Optical (1997).
- [5] F. Shimura, Semiconductor silicon crystal technology, Academic Press, San Diego (1989).
- [6] M. Steinert, J. Acker, K. Wetzig, J. Phys. Chem. C **112**, 14139 (2008).
- [7] A. R. Eyad, A. Ibrahim, A. Hassan, Int. J. Anal. Chem. **2017**, 1 (2017).
- [8] A. V. Narasimha Rao, V. Swarnalatha, P. Pal, Micro Nanosyst. Letter **5**, 1 (2017).
- [9] C. K. Sheng, R. Aarif, E. A. G. E. Ali, M. F. Hassan, J. Sustainability Science and Management, **15**, 6 (2020).
- [10] K. S. Chan, T. J. E. Dwight, Results Phys. **10**, 5 (2018).
- [11] H. Kikuyama, M. Waki, M. Miyashita, T. Yabune, N. Miki, J. Takano, T. Ohmi, J. Electrochem. Soc. **141**, 366 (1994).
- [12] S. K. Milind, F. E. Henry, J. Electrochem. Soc. **147**, 176 (2000).
- [13] F. Nurhaziqah, C. K. Sheng, K. A. M. Amin, M. I. N. Isa, M. F. Hassan, E. A. G. E. Ali, K. H. Kamarudin, R. Aarif, ASM Sci. J. Special Issue **1**, 68 (2018).
- [14] K. L. Shobha, R. L. Min, Himalayan Phys. **2**, 38 (2011).
- [15] C. K Sheng, W. M. M. Yunus, W. M. Z. W. Yunus, Z. A. Talib, A. Kassim, Solid State Sci. Technol. **15**, 16 (2007).
- [16] W. Li, L. Zhou, J. Liu, Digest J. of Nanomaterials and Biostructures. **15**, 375 (2020).
- [17] P. V. Galiy, T. I. Lesiv, L. S. Monastyrskii, T. M. Nenchuk, I. B. Olenych, Thin Solid Films **318**, 113 (1998).